Reflections on glass

James T. Todd

Department of Psychology, Ohio State University, Columbus, OH, USA

J. Farley Norman

Psychological Sciences, Western Kentucky University, Bowling Green, KY, USA

An important phenomenon in the study of human perception is the ability of observers to identify different types of surface materials. The present article will consider a wide range of factors that can influence the perceptual identification of glass, including the structural complexity of an object, whether it is hollow or solid, and the pattern of illumination. Several illumination techniques used in the field of photography are described, and examples are provided to show how they interact with structural complexity. A single psychophysical experiment is reported to evaluate the perceptions of naïve observers using a novel categorization task designed to assess potential confusions among multiple material categories. Finally, the paper will enumerate a number of specific image features that are potentially diagnostic for the identification of glass, and it will evaluate their relative importance for human perception.

Introduction

Since the dawn of civilization, human observers have been fascinated by the appearance of transparent materials such as glass or gemstones. These materials delight the eye by producing complex patterns of refraction and bright highlights that sparkle and shimmer when an object moves relative to the observer or the sources of illumination. The optical properties of glass materials have been studied extensively in the field of physics, but it is somewhat surprising that there is relatively little research in vision science on the perception of glass.

Although there have been a number of studies on how subsurface scattering of transmitted light influences the perception of translucency (Fleming & Bülthoff, 2005; Marlow, Kim, & Anderson, 2017; Motoyoshi, 2010; Xiao et al., 2014), much less is known about observers' perceptions of clear transparent materials. In one of the few experiments on this topic Fleming, Jäkel, and Maloney (2011) showed that subjects can match two glass surfaces against textured backgrounds by adjusting the index of refraction on one of them. This work was later extended by Schlüter and Faul (2014, 2016) who showed that observers can perform this task based on the pattern of specular highlights on a surface without any visible texture in the background. One important limitation of these studies is that the front and back surfaces of the depicted objects had very little curvature, so that refractive distortions were much smaller than those that can arise from glass objects with more complicated 3D structures. Another experiment by Kim and Marlow (2016) used an object with sufficient complexity that the background scene was distorted beyond recognition. Because this object was made of solid glass, it inverted the general coloring of the background so that the blues of the sky were primarily visible in the bottom portion of the object, whereas the greens of the ground were primarily visible in the upper parts. Kim and Marlow argued that this inversion of the background provides useful information for the appearance of transparency. However, it is also important to note that background inversion does not occur for hollow glass objects (e.g., drinking glasses), which are much more common than solid ones in our day-to-day experiences. One last study to be considered in this regard has more recently been reported by Tamura, Higashi, and Nakauchi (2018). They showed that observers can exploit differences in the patterns of optical flow between reflected and transmitted light in order to distinguish between glass and metal surfaces.

One likely reason why there is so little research on the perception of glass is the inherent computational difficulty of creating realistic simulations of glass objects to use as stimuli. During the past decade, there have been dramatic improvements in rendering technology, and a more general availability of fast computer clusters that make it possible to create photorealistic images of complex glass objects without having to wait several days for the render to be completed. Nevertheless, even when one is armed with this

Citation: Todd, J. T., & Norman, J. F. (2019). Reflections on glass. *Journal of Vision*, *19*(4):26, 1–21, https://doi.org/10.1167/19.4.26.

https://doi.org/10.1167/19.4.26 Received September 11, 2018; published April 22, 2019 ISSN 1534-7362

Figure 1. Three photographs of real glass objects.

powerful technology, it is still quite easy to produce images of simulated glass objects that look horribly unnatural, just as it is possible to produce poor depictions of glass in photographs of real objects (Hunter, Biver, & Fuqua, 2007).

The goals of the present article are twofold: First, we will document a wide range of factors that can influence the perceptual appearance of glass using a novel categorization task designed to assess potential confusions among multiple material categories. Second, we will also identify several specific image features that could provide information to distinguish glass objects from other shiny materials, such as metal or obsidian. It is useful to begin this discussion by considering the three photographs of real objects depicted in Figure 1. These include a backlit glass vase, a front lit bumpy glass vase, and a glass sculpture of an elephant illuminated from multiple directions. These are intended to demonstrate how the appearance of glass can vary dramatically among different objects and patterns of illumination, and to provide a benchmark for evaluating the rendered images that will be presented later.

Methods

Material simulations

Almost all of the rendered images presented in this paper were created using the Maxwell Renderer developed by Next Limit Technologies (Madrid, Spain). Maxwell is an unbiased renderer in that it does not use heuristics to speed up rendering times at the cost of physical accuracy. Although the quality of the images it produces is quite high, this comes at a substantial cost in rendering time, especially for materials that involve transparency or translucency. The remaining images were created using the V-Ray renderer developed by Chaos Group (Sofia, Bulgaria), which allowed us to manipulate the number of bounces used for simulating reflections and refractions. The Maxwell images were rendered on a computer cluster with 64 cores, and the rendering times ranged from 30 min to 7 hr depending on the materials, lighting, and the arrangement of surfaces within a scene. The V-Ray images were rendered on a NVIDIA GPU with 300 CUDA cores.

Most of the depicted scenes were illuminated by one of the four HDRI light maps shown in Figure 2. They depict an empty room, an atrium, an esplanade, and an Italian piazza. These maps were all desaturated, and they were sometimes blurred using HDRShop. For other scenes, rectangular area lights were used instead of light maps. The depicted objects were most often positioned on a curved stage that photographers refer to as an infinity curve. This consists of a flat ground plane with diffuse reflectance that curves gradually into a flat back plane. It is designed to give the impression that the background of an object extends to infinity. It is important to note that when an infinity curve is used with an HDRI light map, all the light from below and behind the depicted object is occluded. In some cases the objects were presented without a stage in order to show off the background of the light map. These are the conditions that produced the fastest rendering times.

The Maxwell renderer includes a library of materials with complex indices of refraction (IOR) that vary with wavelength based on published physical measurements of real materials. Most of the images in the present

Figure 2. Four HDRI light maps used to illuminate scenes in the present experiment.

paper depict a Schott crown glass (k7) material from that library (see https://refractiveindex.info/?shelf=glass&book=SCHOTT-K&page=K7). This material has a range of IORs that vary with wavelength from 1.55 to 1.48, and an Abbe number of 60.41. Thus, it produces modest amounts of chromatic dispersion, which appear perceptually as bands of rainbow colors in an image. A few of the images were rendered using a simpler material model with a single IOR of 1.51, and dispersion turned off. The refraction patterns in that case are almost identical to the crown glass except for the color. Three other materials were employed to provide control conditions for the psychophysical experiment. These included a chromium material from the Maxwell library (see https://refractiveindex.info/?shelf=main&book=Cr&page=Johnson), a shiny white material with a linear combination of diffuse and specular components, and a shiny black material (i.e., obsidian), whose reflections were identical to glass, but without any light transmission.

The physics of reflection and refraction

The behavior of light at the boundary between air and glass is governed by the Fresnel equations, which can be used to calculate the percentage of incident light that is reflected or refracted at all possible incident angles and directions of polarization. The effects of polarization will be ignored in the present discussion because natural light is generally unpolarized. The left panel of Figure 3 shows the reflection and refraction curves for light propagating from air to glass, whose IORs are 1.00 and 1.51, respectively. It is important to note that when light flows from air to glass almost all of it is transmitted into the glass except at large incident angles. Thus, surface reflections off glass objects will be primarily visible in peripheral regions near smooth occlusion boundaries, which is where light reflects toward the eye with relatively high incident angles. It is also important to note that reflections off glass tend to be quite dim because glass reflects such a tiny proportion of the incident illumination. Although reflectance increases rapidly at high incident angles, this effect is largely counteracted by the fact that the magnitude of illumination decreases as a cosine function of the incident angle (see Todd & Norman, 2018).

The right panel of Figure 3 shows the reflection and refraction curves for light propagating from glass to air. For small incident angles below 30°, almost all the light flowing from glass to air is transmitted. However, as the incident angle is increased above 30°, the amount of reflection increases rapidly until the angle reaches a critical value of 41°, at which point 100% of the incident light is reflected back into the glass—a phenomenon that is referred to as total internal reflection. The critical angle for total internal reflection varies with the IOR of a material. For water with an IOR of 1.33 it rises to 49°, but for diamond with an IOR of 2.4 it drops to only 25°. The upshot of these effects is that it is

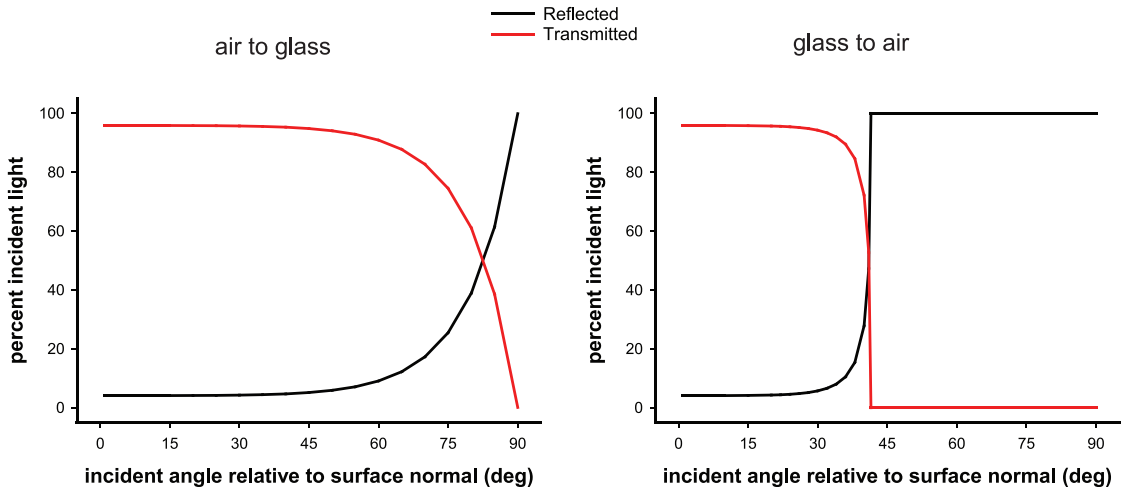

Figure 3. Reflection and transmission as a function of the incident angle from air to glass, and from glass to air.

easy for light to enter glass from air, but it is much harder for it to escape. This is one of the primary reasons why rendering glass materials is so computationally intensive. Once light enters a glass medium, it can bounce around indefinitely before it escapes toward the point of observation. Rendering times are even longer for materials with higher IORs such as diamond or ruby.

To better appreciate the consequences of total internal reflection, it is useful to consider some specific examples. If the light flow inside a glass object were perfectly isotropic, it would be easy to calculate the number of internal bounces required before 99% of its energy is dissipated. For a glass material, 46% of the energy would escape on each bounce, and it would take eight internal bounces before 99% is transmitted back into the air. For a diamond material, only 28% of the energy would escape on each bounce, and it would take 15 internal bounces before 99% of the energy is dissipated. It is important to note that in both of these cases there is a systematic diminishing return for each additional bounce, and most of the energy escapes during the earliest bounces. Of course it is almost never the case that light flow inside a glass object is perfectly isotropic. Within a solid glass sphere, for example, almost all of the internal light flow will hit the surface boundary at a small incident angle, and will therefore escape without any internal bounces at all.

The internal light flow can become much more complex for objects that contain both concave and convex regions. The top row of Figure 4 shows three images of a randomly distorted sphere (see Norman & Todd, 1996; Todd & Norman, 1995) illuminated by the empty room light map in Figure 2. These images were computed using the V-Ray renderer, which makes it possible to control the maximum number of reflective and refractive bounces, and to assign a color (red) to mark the amount of undissipated energy at each pixel that remains after the last bounce. All saturated red pixels mark regions where additional bounces are needed before all available light will escape toward the point of observation, and all desaturated gray pixels mark regions where all of the available light has already escaped. From left to right, the three panels in the upper row of Figure 4 show the results for 5, 10, and 20 bounces, respectively. Note in this case that after 20 bounces almost all of the red in the image has been eliminated. The three panels in the bottom row of Figure 4 show a hollow version of the same object with 10, 40, and 100 bounces, and there is still a small amount of red even after 100 bounces. Hollow objects produce a larger number of internal bounces than solid ones because light becomes trapped inside the glass shell so that most of the rays hit the boundaries at relatively high incident angles that are within the range of total internal reflection. This is the same principle by which fiber optic cables are able to transmit light over long distances.

It is also interesting to note in Figure 4 how the late developing image structure seems to contain nested sets of circular patterns, which appear somewhat similar to the turbulence that can occur in fluid flows. Similar circular patterns are also quite prominent in the photograph of the glass elephant in Figure 1, and many of the other images we will present throughout this paper. For purposes of the present discussion, we will refer to these local swirling patterns as eddies of light flow, or flow eddies. These occur primarily within internally concave regions. Because they seem to be specific to transparent materials, we suspect they could provide a useful source of information for the identification of glass objects. One of the goals of the present experiment was to test that hypothesis by presenting patterns of flow eddies in the absence of other relevant sources of information.

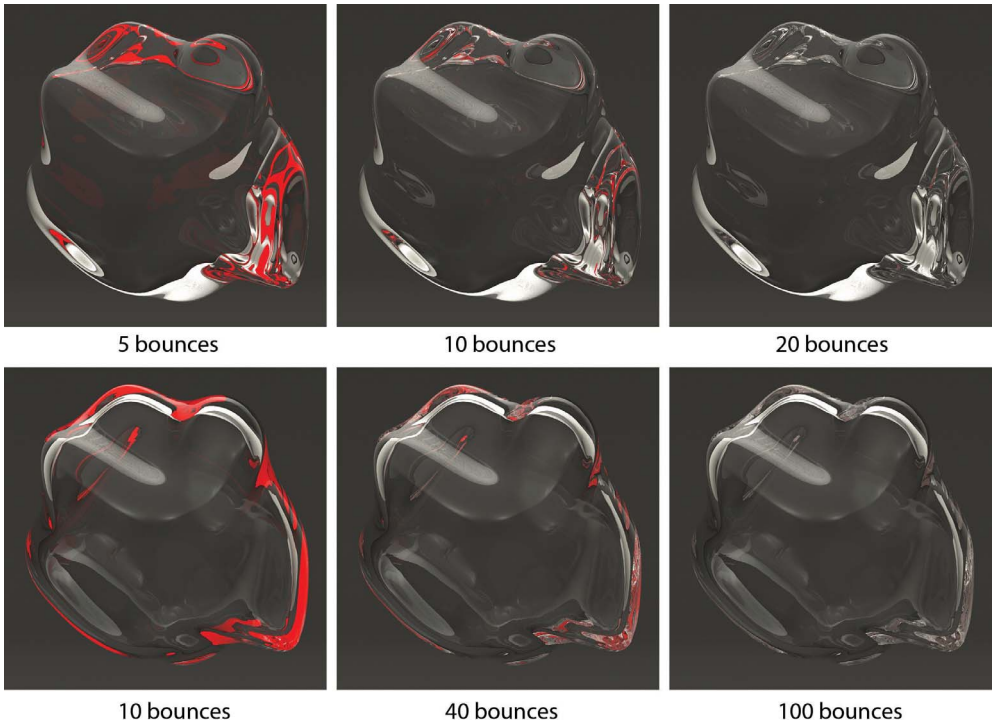

Figure 4. Images of a solid (top) and hollow (bottom) randomly deformed sphere rendered with different numbers of bounces. The variations of red represent the amount of undissipated energy after the maximum number of bounces is completed.

Apparatus

The experimental stimulus images were displayed by an Apple Mac Pro computer (Dual Quad-Core processors, with ATI Radeon HD 5770 hardware-accelerated graphics) using an Apple 27-inch LED Cinema Display (2560 × 1440 pixel resolution). The monitor was located at a 60 cm viewing distance.

Procedure

The experimental stimuli included 80 images depicting a variety of 3D shapes and patterns of illumination. Just under half of these images (38) depicted glass objects because that was the main focus of the experiment. Control stimuli included 10 objects with a metal material, 10 objects with a shiny black material, 10 objects with a shiny white material, and 12 images of glass or a shiny black material that were modified in Photoshop by edge filtering or changing the background in order to alter their perceptual appearance.

On each trial, observers were presented with a single image and were required to categorize the depicted material by adjusting four sliders with a hand-held mouse. Each of the sliders represented a different category labeled glass, metal, shiny black, or something else, and a digital readout was also provided for each one. Observers were instructed to adjust the sliders to indicate their confidence rating for each of the four possible categories. These confidence ratings were constrained by the program so that the four different ratings would always sum to 100%. We knew from our own informal observations that images of glass can occasionally be misinterpreted as a metal or shiny black material. That is why we included the metal and shiny black control stimuli, and incorporated those categories in the response settings. However, we did not want the observers to feel forced to only consider glass, metal, or shiny black when evaluating each stimulus, so we also included a "something else" response option, and also added the shiny white control stimuli in an effort to force them to give that category a high rating on a subset of the trials.

Observers

The displays were judged by one of the authors (JFN) and eight other observers who were completely naïve about the purpose of the experiment or how the displays were generated. All observers possessed normal or corrected-to-normal visual acuity. Observers made judgments for all 80 stimuli in a single experimental session. At the beginning of each session, the details of the response task were explained, and observers were shown real physical examples of glass, metal, and shiny black materials. However, they were also instructed that other types of materials would be presented as well, and that those should be categorized as something else.

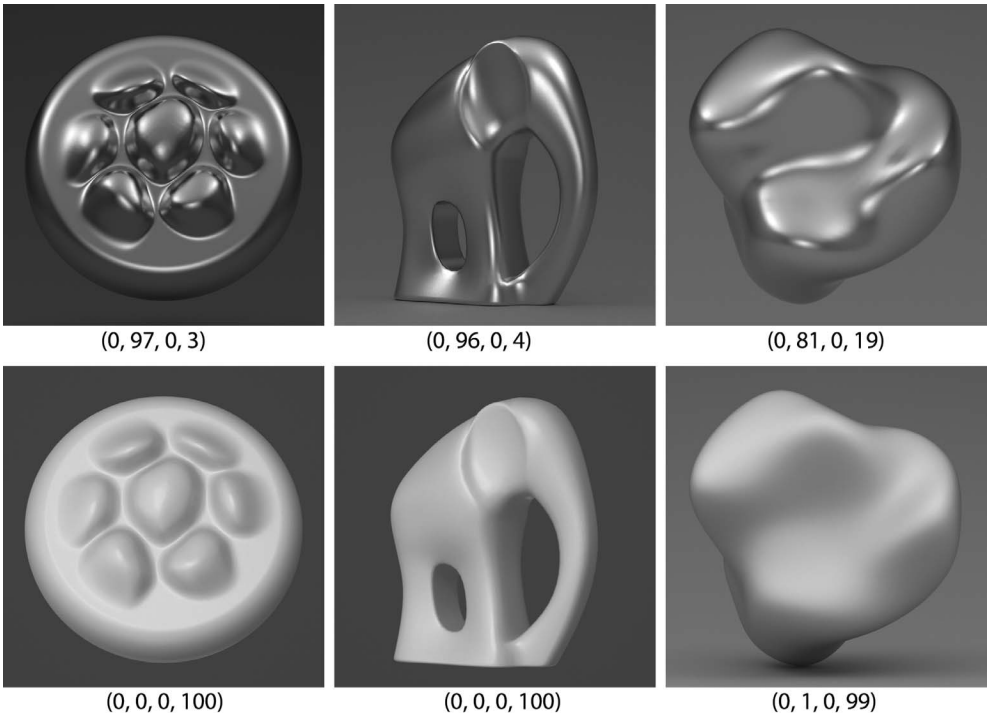

Figure 5. Six of the control images from the present experiment. The ones in the top row depict metal (chrome) objects, whereas the ones in the bottom row have a shiny white material. The average categorization ratings for the nine observers are shown just below each image. From left to right, the numbers in parentheses represent the average confidence rating for glass, metal, shiny black, and something else, respectively.

Results

Let us first consider the results obtained from the control stimuli. The top row of Figure 5 shows three example images of metal objects, and the bottom row of that figure shows three examples of the shiny white objects (examples of the shiny black objects will be shown later). The average categorization ratings for the nine observers are shown just below each image. From left to right, the numbers in parentheses represent the average confidence rating for glass, metal, shiny black, and something else, respectively. The overall pattern of results revealed that the control stimuli achieved their intended purpose in that the metal stimuli were categorized as metal with an average confidence rating of 90%, the shiny black stimuli were categorized as shiny black with an average confidence rating of 93%, and the shiny white stimuli were categorized as something else with an average confidence rating of 99%.

It is important to keep in mind when evaluating these data that the response scale had a fixed upper and lower limit of 0% and 100%, respectively, and that most of the responses were clustered near those endpoints. This indicates that observers were generally quite confident about which of the possible response categories was most appropriate for most of the depicted stimulus objects. However, this clustering of responses near the endpoints complicates an analysis of confidence intervals, because it forces the variance of the observers' judgments to covary systematically with the mean. For example, 69% of the average confidence ratings were between 90%–100% or 0%–10%, and the average standard error for those ratings was only 1.03%. Of the remaining responses, 24% had average confidence ratings between 70%–90% or 10%–30%, and the average standard error for those was 6.97%. Only 7% had an average confidence rating between 30%–70%, and the average standard error for those was 12.65%. In other words, when observers expressed high confidence in their categorization judgments, the variance among different observers was extremely low, but the variance among observers increased sharply for the smaller proportion of stimuli in which the ratings were more evenly distributed across two or more categories.

The effects of structural complexity

Within the eighty experimental images, there were five that depicted spherical objects illuminated by the atrium light map (see Figure 2). These are all shown in Figure 6, and the average categorization ratings for the nine observers are shown just below each one. From

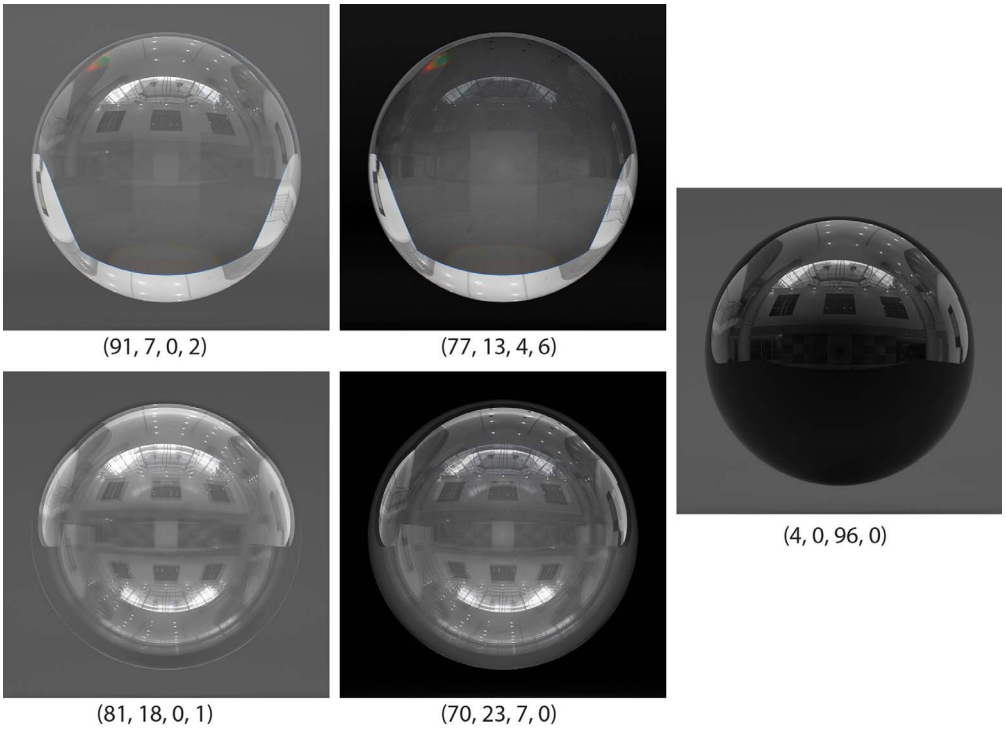

Figure 6. Five images of a spherical object in different conditions. The images in the left column depict a solid glass object on the top and a hollow one on the bottom. The specular reflections from these images are shown in isolation in the right panel. The images in the two middle panels show the transmitted light presented in isolation. The average categorization ratings for the nine observers are shown just below each one. From left to right, the numbers in parentheses represent the average confidence rating for glass, metal, shiny black, and something else, respectively.

left to right, the numbers in parentheses represent the average confidence rating for glass, metal, shiny black, and something else, respectively. The images in the left column depict a solid glass object on the top and a hollow one on the bottom. Note that the specular reflections off the outer surface are exactly the same for both of these objects. Those reflections are shown in isolation in the right panel that depicts a shiny black material with the same IOR as glass, but without any light transmission. The images in the two middle panels were obtained by subtracting the image on the right from the two on the left, which reveals the transmitted light presented in isolation. Because we obtained ratings in all of these conditions, it is possible to assess the relative contribution of reflected and transmitted light on observers' perceptions. When surface reflections on a sphere are presented in isolation, observers rate the material as shiny black with a very high confidence. When transmitted light from a sphere is presented in isolation, the material is judged as glass, but with noticeably less confidence than when reflections and refractions are combined, and the ratings suggest that they appear slightly metallic.

Surfaces of constant curvature like planes or spheres are very special cases, because they produce predictable patterns of reflection and refraction with relatively little distortion. Consider the image of the solid glass sphere in the upper left panel of Figure 6. Note the reflections of the sky light and the recessed lighting of the atrium on its top half, and a brighter and more compressed pattern of refraction near the bottom. The hollow sphere on the bottom left has a more complicated pattern, with two upright reflections of the atrium on the top from the inner and outer boundaries of the front surface, and two inverted reflections on the bottom (after three bounces) from the inner and outer boundaries of the back surface. The key thing to note in these images of a sphere is that the structure of the surrounding scene is clearly recognizable in both the patterns of reflection and refraction. That is not the case for objects with more complex 3D structures, which could perhaps suggest that psychophysical results obtained with spheres may not generalize to other situations.

It is useful to contrast the images of a sphere with the ones in Figure 7 that depict a spherical object that has been transformed by a series of sinusoidal deformations (see Norman & Todd, 1996; Todd & Norman, 1995), and illuminated by the atrium light map. The overall organization of this figure is the same as Figure 6. The images in the left column depict a solid glass object on the top and a hollow one on the bottom; the one on the right shows the outer surface reflections of these objects presented in isolation; and the transmitted light from

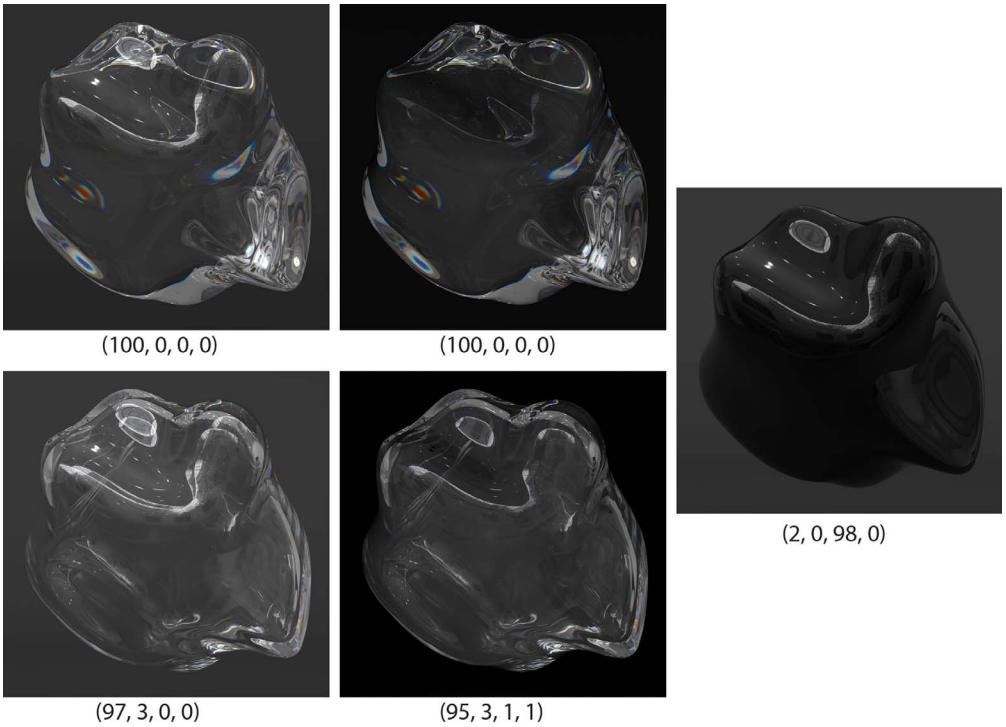

Figure 7. Five images of a randomly deformed sphere in different conditions. The images in the left column depict a solid glass object on the top and a hollow one on the bottom. The specular reflections from these images are shown in isolation in the right panel. The images in the two middle panels show the transmitted light presented in isolation. The average categorization ratings are shown just below each image. From left to right, the numbers in parentheses represent the average confidence rating for glass, metal, shiny black, and something else, respectively.

each object is presented in isolation in the middle column. The numbers in parentheses below each image show the average confidence rating for glass, metal, shiny black and something else, respectively.

It is important to note in these images that the structure of the surrounding scene is no longer recognizable in the patterns of reflection and refraction, yet observers can still identify the depicted materials and have a clear perception of the overall 3D shape. Indeed, the observers categorized these images with an average confidence rating of 98%. The isolated reflections were categorized as shiny black, and all of the others were categorized as glass. The informative optical structure about glass in these examples arises from light that is transmitted into the object from the top, sides and front. Consider the image of a solid deformed sphere in the upper left panel of Figure 7. There is a sharply curved ridge on the lower right of that object, which contains some very bright highlights. These are not specular reflections, as is easily verified by comparing this image to the one of obsidian in the right panel. From the perspective of the inside, this region is a narrow and deep concavity that is particularly effective at trapping light (see Figure 4), and the multiple internal reflections this produces greatly increase the probability that light can escape that region toward the point of observation. It is also interesting to note how the visible light from that region contains numerous flow eddies, which are also clustered around the three bumps at the top of the object. It is likely that these structures provide the critical information for the confident identification of glass in these images, especially in the case where the specular reflections have been removed.

The lower left panel of Figure 7 depicts a hollow, deformed sphere. Note there is a brightening of the glass shell along most of the object's perimeter and that this produces a visible contour that separates the inner surface of the glass shell from the hollow center. We shall refer to these features as solid/hollow boundary contours, and they provide a powerful source of information for the identification of glass materials and the appearance of hollowness. Other information to support that impression is provided by the pattern of double reflections from the inner and outer boundary. The flow eddies are less prominent in this image, and they are confined primarily to the glass shell along the periphery.

The deformed sphere in Figure 7 has a more complex structure than a sphere, but it is still relatively simple compared to many other objects encountered in the environment, like the bumpy glass vase shown in Figure 1. The upper left image of Figure 8 shows a spherical object with a large number of bumps, and illuminated by the esplanade light map in Figure 2. The

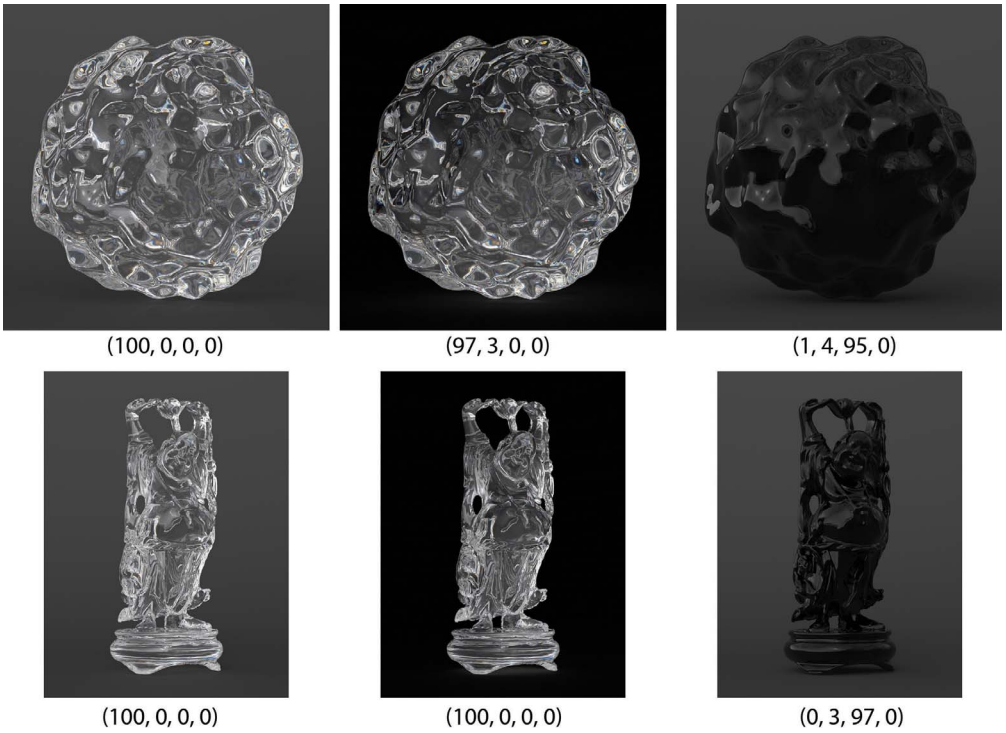

Figure 8. Images of a bumpy sphere and a statue of the Buddha. The images in the left column depict solid glass objects. The specular reflections from these images are shown in isolation in the right column. The images in the two middle panels show the transmitted light presented in isolation. The average categorization ratings are shown just below each image. From left to right, the numbers in parentheses represent the average confidence rating for glass, metal, shiny black, and something else, respectively.

lower left image shows a statue of the Buddha illuminated by the esplanade light map. The images in the right column show the outer surface reflections of these objects presented in isolation, and the ones in the middle column show the transmitted light presented in isolation. Most researchers in the perceptual analysis of image shading would likely conclude that these surfaces are covered with a dense pattern of specular highlights, but that is not the case. The specular reflections on these objects are identical to the ones shown in the right column. What appear to be bright highlights on the glass are actually caused by the light flow inside the object. The regions that appear bright are those where light is channeled in just the right direction so it is transmitted across the boundary toward the point of observation. It is also interesting to note in this regard that light tends to get trapped inside the internally concave regions, so that there are numerous flow eddies, with circular bands around many of the visible bumps. This creates a kind of visual texture that is unique to bumpy glass objects. The fact that observers can categorize these objects as glass with 100% confidence when the transmitted light is presented in isolation provides especially strong evidence that flow eddies are a powerful source of information. This is because in that particular case they are the only source of information that is available.

The effects of illumination

Any professional photographer will acknowledge that the appearance of glass in an image is critically dependent on the pattern of illumination. In this section we will show how the effects of illumination can strongly interact with the effects of structural complexity. Let us begin by considering the perceptual effects of indirect light from a background scene. From the limited psychological literature on the perception of glass (Fleming et al., 2011; Schlüter & Faul, 2014, 2016; Khan, Reinhard, Fleming, & Bülthoff, 2006; Kim & Marlow, 2016), one could easily get the impression that refractive distortions of background textures provide a critical source of information. However, if one does a Google image search for "glassware," almost none of the images that are found will have any structured background at all. Could the photographers who created these images know something that perceptual psychologists do not? Most of the images that pop up on a glassware Google search were created for product visualization. Background textures are generally avoided in that context because they divert attention from the glassware itself, and are not at all necessary to provide compelling information about glass materials.

Figure 9 shows images of a glass sphere (left) and a distorted glass sphere (middle) presented against a

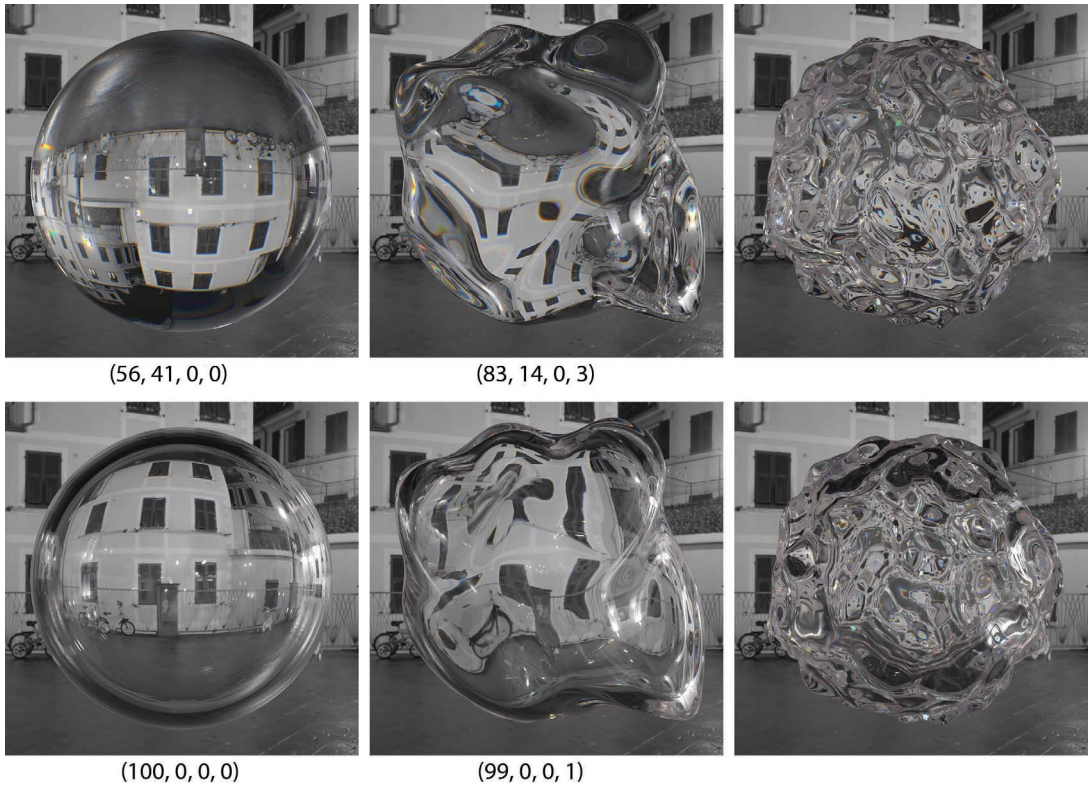

Figure 9. Images of three objects against a background scene of an Italian piazza. The images in the top row are solid, whereas the ones in the bottom row are hollow. The average categorization ratings are shown just below each image. From left to right, the numbers in parentheses represent the average confidence rating for glass, metal, shiny black, and something else, respectively.

background image of an Italian piazza (see Figure 2). The objects depicted in the top row are solid, whereas the ones in the bottom row are hollow. The numbers in parentheses below each image show the average confidence rating for glass, metal, shiny black and something else, respectively. Note how the background scene appears right side up through the hollow objects, and upside down through the solid ones (see Kim & Marlow, 2016). There appears to be an interaction in these data between the background texture and the solidity of the depicted object. For the hollow objects, the observers' glass confidence ratings were as high or higher than those produced by the same objects in Figures 6 and 7 with a uniform gray background, but for the solid objects with a background texture these ratings were substantially lower than those produced with a uniform background. One possible reason for this is that the images of hollow objects contain additional information from the solid/hollow boundary contour along the periphery of each object.

The right column of Figure 9 shows solid and hollow versions of the same bumpy sphere depicted in Figure 8. Although these images were not presented in the psychophysical experiment, they are included here to demonstrate how refractive distortions can completely destroy the coherent structure of the background for objects that are sufficiently complex. Note in particular how these distortions have transformed the background into a complex pattern of flow eddies that appears remarkably similar to the one in Figure 8 where the same object is presented against a uniform background. Another interesting thing to note in the hollow bumpy sphere is that it is difficult to discern a solid/hollow boundary contour, which could explain why that object does not appear hollow.

In the popular book on photographic lighting by Hunter et al. (2007, p. 149), there is a chapter on transparent materials titled "The case of the disappearing glass." It begins with the following observation: "The distant genius who first fused sand into glass has tricked the eyes and delighted the brains of every generation of humans to follow. It has perhaps also grayed the hair and wasted the time of more photographers than any other substance." Consider the image shown in Figure 10 that depicts four drinking glasses against a black background illuminated by a rectangular area light positioned just above the point of observation. This image is a disaster from a photographic perspective, primarily because there is little or no light along the boundary of the objects that is reflected or transmitted toward the point of observation. As a result of that problem, the contours of the objects are mostly invisible.

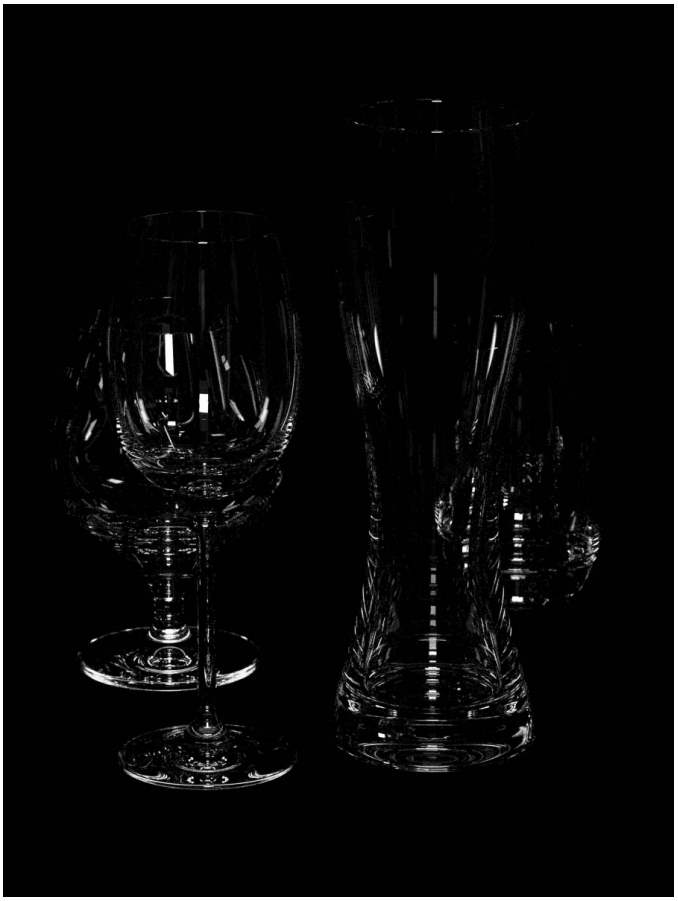

Figure 10. An image of four glasses illuminated by a single area light against a dark background.

This problem could be mitigated to some extent by using colored glass or presenting the objects against a textured background to create a color or texture contrast along the boundaries. However, there are many photographic contexts where neither of those solutions is acceptable. In order to avoid problems with edge definition, photographers have worked out two classic illumination strategies that are often referred to as the bright-field method and the dark-field method. In order to understand the logic of these approaches, it is important to recognize that there is only a narrow range of illumination directions for which regions along an object's boundary will reflect any light toward the point of observation. The secret to good edge definition is to control the light along those critical directions. In the bright-field method there is no illumination in the critical directions so that the edges are dark, and the object is presented against a white background so that everything else is light. The dark-field method is exactly the opposite: The illumination is focused in the critical directions so that the edges are bright, and the object is presented against a black background so that everything else is dark (see Bousseau, Chapoulie, Ramamoorthi, & Agrawala, 2011).

The bright-field method is the one that was employed in the photograph of a glass vase in the left panel of Figure 1, and it is by far the most common pattern of illumination in the images that pop up on a Google search for "glassware." The left panel of Figure 11 demonstrates this approach using the same set of glasses as in Figure 10, but with diffuse back illumination. These objects are presented on an infinity curve, and there is a single rectangular area light behind the objects to illuminate the backplane. Because the infinity curve has a Lambertian reflectance function, the objects are illuminated indirectly with diffuse light from behind, and this produces a perceptually compelling appearance of glass without any specular reflections or refractive distortions of a background texture. This image was categorized as glass in the present experiment with an average confidence rating of 99%. Note that all of the objects depicted in this scene have a hollow top on a solid base, and that they all exhibit a solid/hollow boundary contour at the interface between those regions. These provide a powerful source of information for the identification of

Figure 11. Images of objects with diffuse illumination from behind. The left and middle objects are hollow, whereas the one on the right is solid. The average categorization ratings are shown just below each one. From left to right, the numbers in parentheses represent the average confidence rating for glass, metal, shiny black, and something else, respectively.

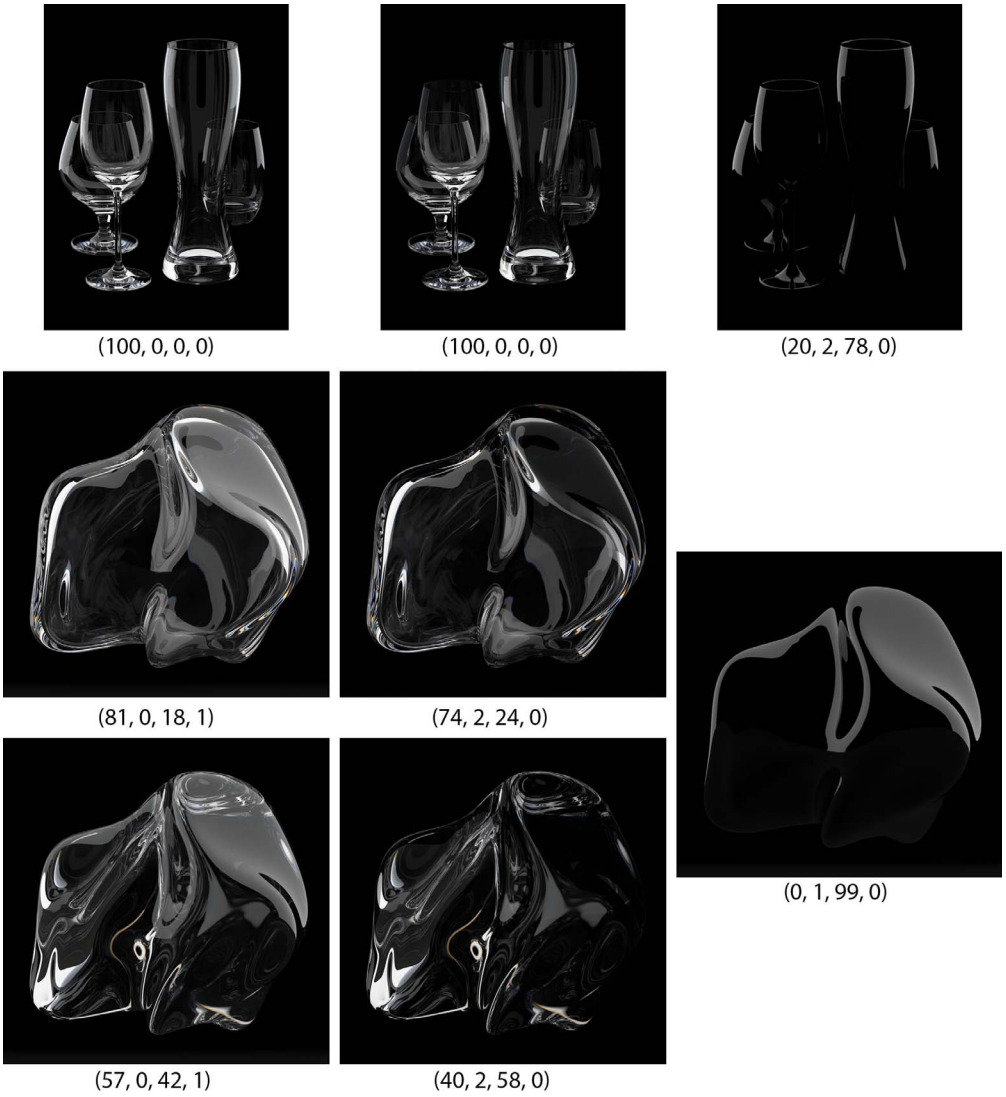

Figure 12. Images of objects with diffuse illumination from the periphery. The left column depicts hollow objects in the top and middle panels, and a solid object in the bottom panel. The specular reflections from these images are shown in isolation in the right column, and the transmitted light is shown in isolation in the middle column. The average categorization ratings are shown just below each image.

glass materials (and hollowness), as does the overall configuration in which the contours of the two back objects are visible through the two front ones.

The bright-field method works exceptionally well with glassware, which is why it is so popular with photographers. However, it can be less effective with more complex shapes, especially those composed of solid glass. For example, the middle and right panels of Figure 11 show a randomly deformed sphere with the same illumination as in the left panel. The one in the middle depicts a hollow object. Observers judged this as glass with a reasonably high confidence (80%), but it also appears slightly metallic (20%). Although there are some flow eddies in that image, another relevant source of information is provided by the solid/hollow boundary contour that separates the inner surface of the glass shell from the hollow center. The image on the right depicts a solid version of the same object, and the glass confidence rating for that was only 52%. Although there are very prominent flow eddies in this image, observers may have had difficulty interpreting the large white areas that are brighter than the background. These observations suggest that the effectiveness of diffuse back lighting may be primarily limited to hollow objects.

One way of implementing the dark-field method is to illuminate objects from the periphery against a black background, which also has the added advantage of producing images with a high degree of drama. Figure 12 shows three examples of this technique. All of the depicted objects were illuminated from behind by a large area light, with an opaque black panel to block

this light from the camera's field of view. The net result of this setup is that the unoccluded portions of the area light illuminate the scene from the periphery, which produces bright boundary contours that stand out from the black background. The left column of this Figure 12 shows the same three scenes that are depicted in Figure 11; the right column shows the outer surface reflections of these objects presented in isolation; and the transmitted light from each object is presented in isolation in the middle column. The numbers in parentheses below each image show the average confidence rating for glass, metal, shiny black, and something else, respectively.

The overall pattern of results is similar to those obtained with the bright-field method. All nine observers categorized the glassware as glass with 100% confidence; the ratings dropped to 81% for the hollow deformed sphere; and they dropped even lower to 57% for the solid object. One interesting difference from the bright-field images is that the primary confusion was shiny black rather than metal. If the images in the left column were presented on their own, they could easily be interpreted as if the appearance of glass is due entirely to specular reflections, but that interpretation would be incorrect. What appear to be bright reflections on the glass are mostly caused by the light flow inside the object. Indeed, when the specular reflections are presented in isolation, they are perceived with high confidence as a shiny black material. Conversely, when the transmitted light is presented in isolation, the glass confidence ratings are only slightly lower than when reflections and refractions are presented in combination.

The sources of information for identifying the glass materials in Figure 12 are the same ones that are available in Figure 11. For the left and middle images of four glasses there are solid/hollow boundary contours between the base of each object and its hollow top, and the contours of the two back objects are visible through the front ones. Note that neither of these features is present when the specular reflections are presented in isolation, and that image was categorized as shiny black. For the hollow deformed sphere there is a solid/hollow boundary contour that separates the inner surface of the glass shell from the hollow center, together with a number of small flow eddies. For the solid deformed sphere there are numerous large flow eddies, but they do not provide sufficient information in this context to allow a confident identification of the glass material.

From the examples provided thus far, it seems to be the case that solid glass objects do not always provide sufficient information for a confident identification of glass materials. Most observers have relatively little experience with clear solid glass objects, unless they are collectors of glass sculpture. Consider the photograph of a solid glass elephant in the right panel of Figure 1, and pay particular attention to the bright regions on the ground along its base. These bright spots are called caustics, and they are caused by light that illuminates a surface after being transmitted through a transparent object. From the number of caustics in this image it is clear that the object was illuminated from multiple directions. Studio photographers often use multiple lights to illuminate a subject, and they will frequently adjust the placement of those lights to get just the right look they are trying to achieve.

The images presented in Figure 13 were designed in an effort to simulate this process. The Maxwell renderer has a very convenient feature that allows one to populate a scene with a large number of lights, and then adjust their relative intensities in real time after the render is completed, to find just the right combination. The image in the upper left panel depicts a solid glass object on an infinity curve illuminated by seven small area lights (culled from a larger set of 30) pointing towards the object in different directions and with different relative intensities. These were chosen through trial and error in order to maximize the appearance of glassiness. The right panel shows the outer surface reflections of this object presented in isolation, and the transmitted light is presented in isolation in the middle panel. The observers' confidence ratings are shown in parentheses below each image. One perplexing aspect of these data is that observers' confidence ratings for the left and middle images of Figure 13 were almost twice as high as those obtained with the same solid object in Figures 11 and 12, with a very similar pattern of flow eddies. We suspect this may have something to do with contrast relations among various regions, but we have not been able to formulate a specific hypothesis about that.

Although the image in the upper left panel of Figure 13 was categorized as glass with 100% confidence, its abrupt changes in contrast and sharp internal edges seem a bit stark for our aesthetic tastes. The image in the lower left panel was designed to correct these flaws using another technique borrowed from photography. That scene included a hemispherical translucent tent. The depicted object and the camera were on the inside of the tent, and the area lights were on the outside. Filtering the light sources through a tent effectively eliminates the glaring dark regions in an image and smooths out the bright highlights, resulting in a much softer perceptual appearance.

The use of a translucent tent in computer graphics can greatly increase rendering time. There is, however, a much more efficient technique for softening the illumination, which is not available to photographers. The primary effect of the tent is to blur patterns of illumination, but this can be achieved more easily using an HDR image editor (e.g., HDRShop) to create

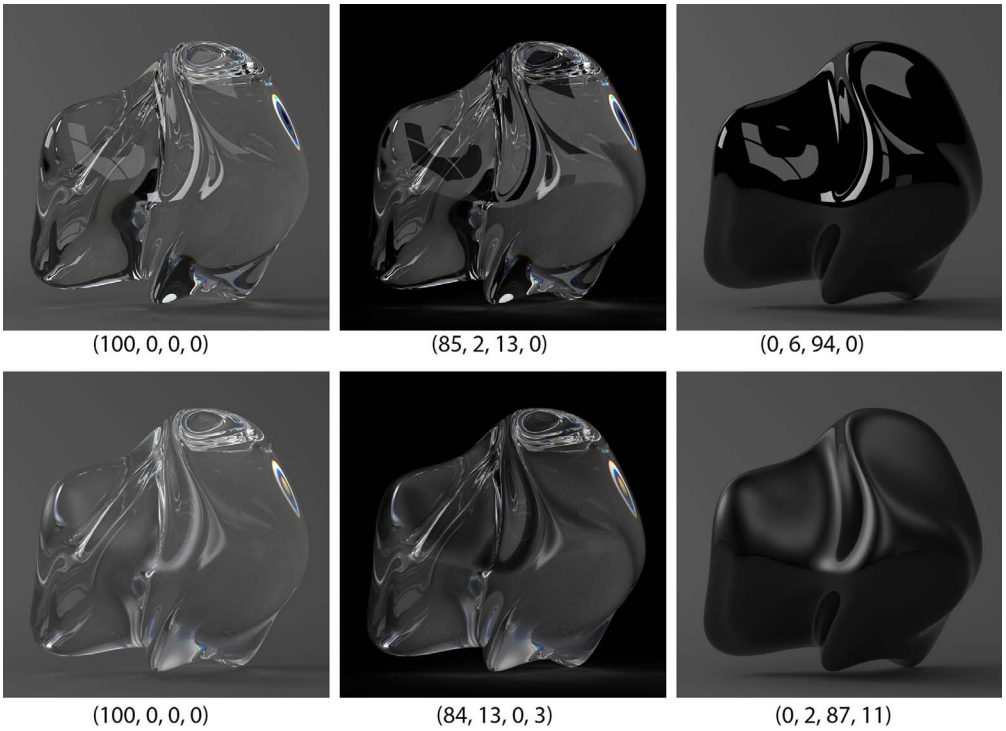

Figure 13. Images of a single object with different patterns of illumination. The object in the top left panel was illuminated by seven small area lights. The same lights were used in the bottom left panel except that they were filtered through a hemispherical translucent tent. The specular reflections from these images are shown in isolation in the right column, and the transmitted light is shown in isolation in the middle column. The average categorization ratings are shown just below each image. From left to right, the numbers in parentheses represent the average confidence rating for glass, metal, shiny black, and something else, respectively.

blurred light maps (see Doerschner, Boyaci, & Maloney, 2007). The left column of Figure 14 shows three objects illuminated by the esplanade light map shown in Figure 2. These objects are all suspended in empty space, and are illuminated from all directions, because there are no background surfaces to occlude the light. This creates a finely detailed texture in the patterns of reflection and refraction that appears quite distracting. The middle column of Figure 14 shows the same objects illuminated by a blurred version of the same light map. Note how this smooths out the texture without impairing the perceptual identification of the glass material. The right column of Figure 14 shows the same set of objects with an unblurred light map, but with a small amount of roughness added to the material as typically occurs with frosted glass. Note that the presence of surface roughness blurs the visible texture from the light map, but it also severely reduces the observers' confidence that the depicted material is glass. This finding indicates that for the perception of glass materials, observers can somehow distinguish the effects of blurring the pattern of illumination from the blurring that is caused by the microscopic scattering of light on rough surfaces. This result is especially interesting because those different types of blurring are perceptually equivalent for matte materials (Doerschner et al., 2007).

The effects of image contours and contrast polarity

In our discussion of the images presented thus far, we have identified two types of low-level information that could potentially be used for the perceptual identification of glass materials. The first type of structure consists of swirling bands of contours that we have referred to as eddies of light flow. As is demonstrated in Figure 4, these structures develop over multiple bounces inside a glass material, and they are particularly prominent for solid glass objects that contain both concave and convex regions. The other type of structure involves the contours that occur at the boundaries between hollow and solid regions. For example, most of the glassware produced for human use has a hollow top on a solid base and there is typically a visible contour at the boundary between them (e.g., see Figures 11 and 12). A similar phenomenon occurs for completely hollow objects. If the glass shell is sufficiently thick, then a visible contour will appear along the internal boundary of the shell (e.g., see Figures 4, 6, 7, 9, 11, and 12).

In designing our psychophysical experiment, we were curious if observers could identify glass materials from contour structures presented in isolation without any

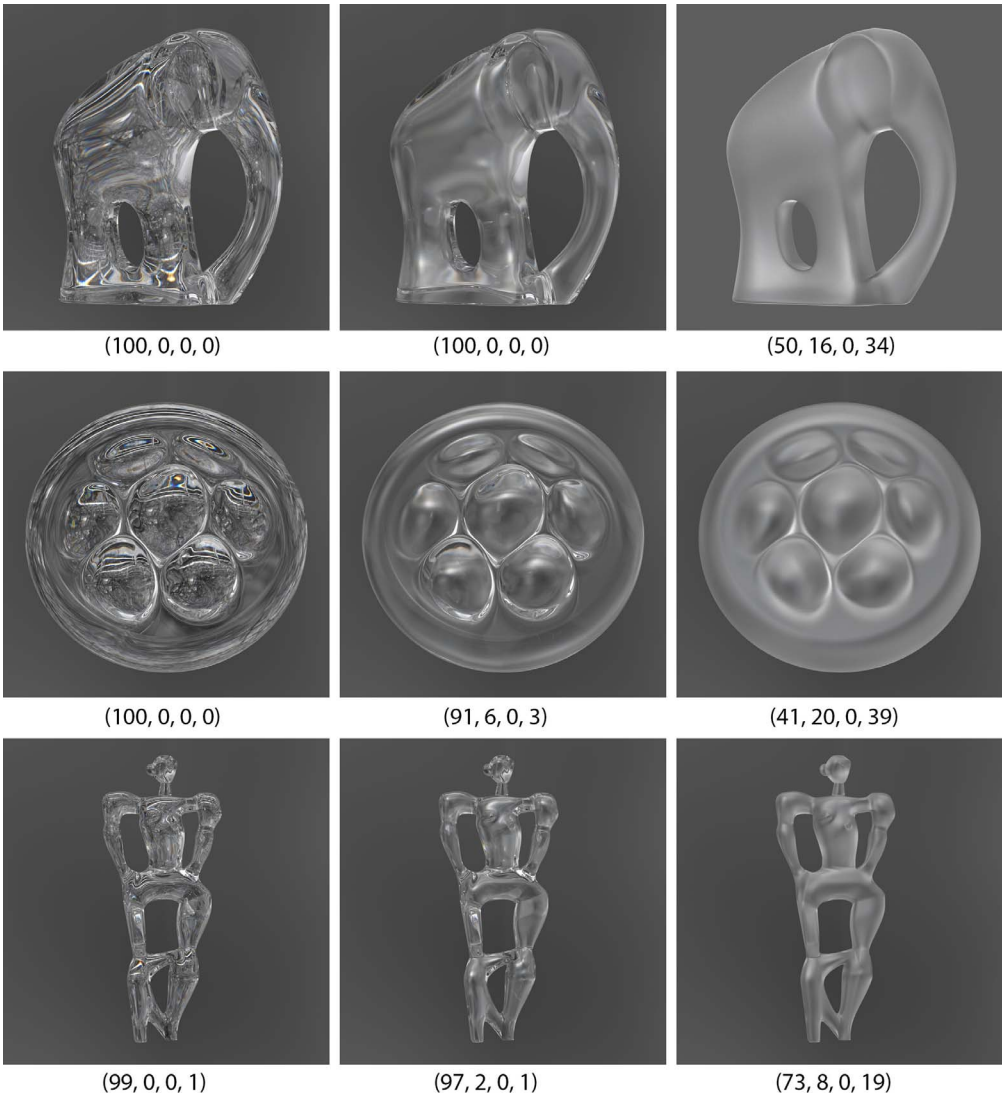

Figure 14. Images of three objects with different illumination and roughness. The objects in the left column are illuminated by the esplanade light map, and the ones in the middle column are illuminated by a blurred version of that same light map. The illumination depicted in the right column is the same as on the left, but the depicted glass materials have a small amount of roughness. The average categorization ratings are shown just below each image. From left to right, the numbers in parentheses represent the average confidence rating for glass, metal, shiny black, and something else, respectively.

other variations in gray scale. In order to address this issue, we transformed the left and middle images of Figure 11 and the upper middle image of Figure 14 using the Photoshop edge finder. The set of four glasses from Figure 11 were reduced to two so there would be no contours of one glass seen through another. The outputs of this filter were then inverted so that the contours would appear as white on black, and the brightness was adjusted so that they would all be clearly visible. The resulting images are shown in the upper row of Figure 15, and the numbers in parentheses below each one show the average confidence rating for glass, metal, shiny black, and something else, respectively. As a control condition, we also created transformed images of the same objects composed of obsidian with frontal illumination so that all the contours resulted from surface reflection rather than transmission. Those images are shown in the lower row of Figure 15.

The results from these images revealed that the contour patterns derived from glass materials were categorized as glass with an average confidence rating of 92%, whereas those derived from obsidian were categorized as glass with a confidence rating of only 60%. We were somewhat surprised by that latter result, because obsidian materials are reliably perceived as shiny black when all grayscale information is available. Nevertheless, this finding provides clear evidence that observers can reliably distinguish the contours in an image that arise from the reflection and transmission of

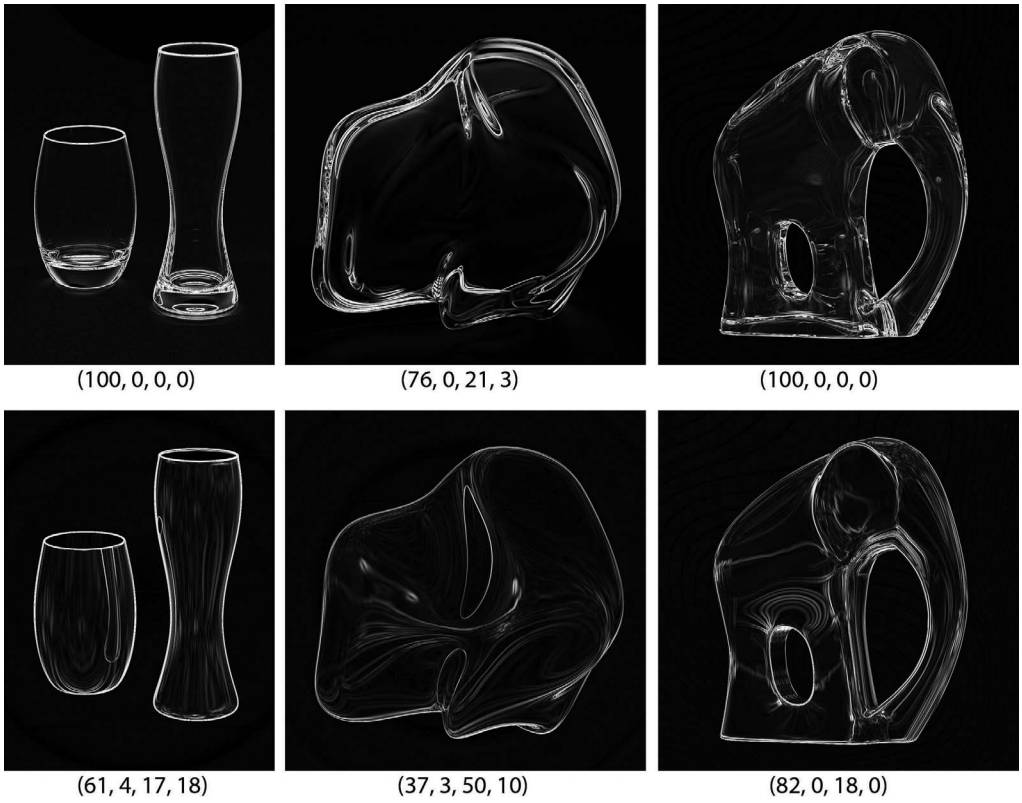

Figure 15. The extracted contours of six images. The contours in the top row were obtained from images of glass, whereas those in the bottom row were obtained from images of obsidian. The average categorization ratings are shown just below each image. From left to right, the numbers in parentheses represent the average confidence rating for glass, metal, shiny black, and something else, respectively.

light. An important property of these images is that they were all composed of white contours on a black background with very high contrast. This gives the depicted objects an apparent sparkle that greatly facilitates the perception of glass. In piloting this study we observed that the apparent glassiness is greatly reduced if the contours are presented as black on white.

It has long been known that there are physical and perceptual constraints on the relative contrasts of neighboring image regions for the appearance of transparency within overlapping planar patches (e.g., Beck, Prazdny, & Ivry, 1984; Metelli, 1970, 1974; Singh & Anderson, 2002), and we wondered whether similar constraints might also influence the material identification of 3D glass objects. In order to address this issue, we took six of the images of glass from Figures 8, 11, 12, 13, and 14, and we altered the color of the background using Photoshop. If the original image had a light background, it was changed to black, and if it had a dark background, it was changed to white. These transformed images are shown in Figure 16, and the observers' confidence ratings are shown below each one. The three objects in the top row of this Figure were all identified as glass, but the confidence ratings were 4%–42% lower than those obtained for the unmodified original images. These reductions were even larger for the objects in the bottom row (i.e., 50%–64%), and those objects were primarily categorized as a metal or shiny black material. This is a remarkable finding. By simply changing the background color of an image, it is possible to alter the perceived material category of an object from glass to metal or glass to shiny black. We suspect this may be a useful procedure for future research in order to assess the relative salience of different sources of information for the identification of glass materials.

Discussion

Let us now consider a variety of factors in the structure of visual images that could conceivably be useful for the identification of glass materials. One such factor that has been mentioned in previous work on this topic is the pattern of specular reflections (Fleming et al., 2011; Schlüter & Faul, 2014, 2016). Although specular reflections are often visible on glass surfaces, our results suggest they may have minimal impact on the perceptual identification of glass. It is important to

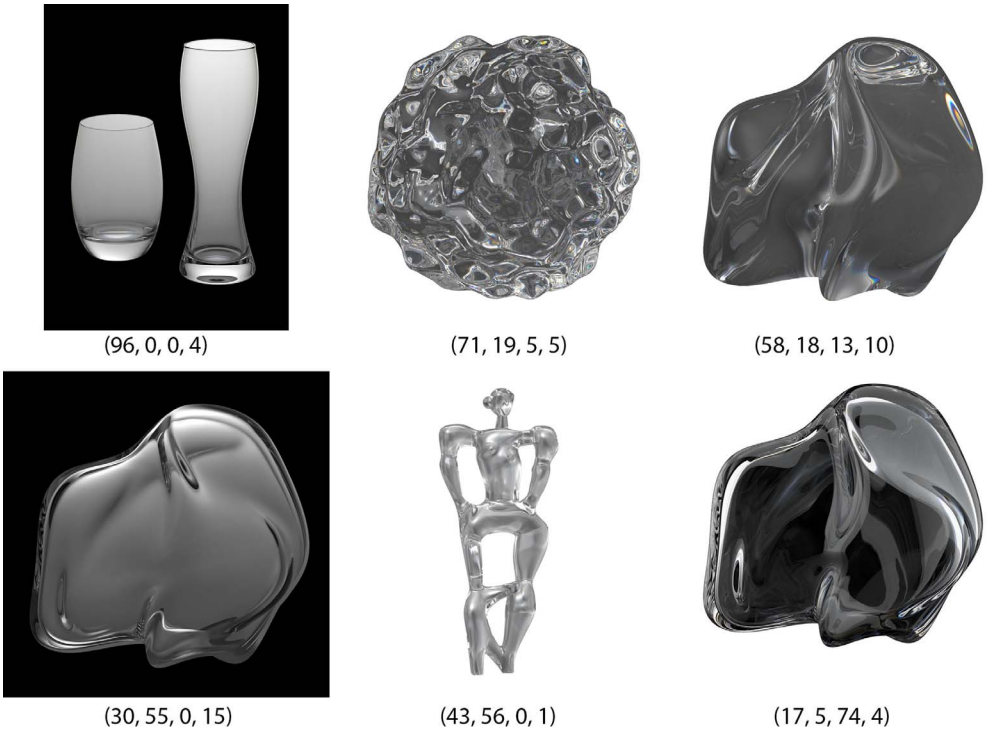

Figure 16. Modified versions of six images whose backgrounds have been altered to violate classical constraints on transparency. The average categorization ratings are shown just below each image. From left to right, the numbers in parentheses represent the average confidence rating for glass, metal, shiny black, and something else, respectively.

keep in mind that shiny black surfaces (e.g., obsidian) reflect light in exactly the same way as glass (Todd & Norman, 2018). When these reflections were presented in isolation in the present experiment, they were rated as shiny black with an average confidence of 93%, whereas the average glass confidence rating was only 3%. When transmitted light was presented in isolation, observers categorized the depicted material as glass with an average confidence of 84%, which is only slightly lower than the 92% confidence they expressed when reflected and transmitted light were presented in combination. It is also interesting to note in this regard that professional photographers often eliminate specular reflections altogether by illuminating glass from behind (see Hunter et al., 2007).

Another potentially relevant source of information that has been discussed in the literature includes distortions of background textures. Fleming et al. (2011) and Schlüter and Faul (2014, 2016) have provided some compelling demonstrations to show the effects of background distortions on the perception of glass. Our results suggest that there may be a complex interaction between background distortions and the 3D structure of the depicted object. For the solid objects with a background scene shown in Figure 9, the observers' glass confidence ratings were substantially lower than those obtained with a uniform gray background. However, for the hollow objects, the presence of a background scene produced confidence ratings that were as high or higher than those that were obtained with a uniform gray background. This is probably because there is additional information from the solid/hollow boundary contour at the interface between the inner surface of the glass shell and the hollow interior. If a depicted object is sufficiently complex, the refractive distortions of a background scene can become completely uninterpretable (see right column of Figure 9), and are perceived as a dense, high frequency texture rather than a distorted scene. It is also interesting to note that the structure of this texture bears a striking resemblance to the patterns of flow eddies on bumpy surfaces (see Figure 8).

The contours that are formed within images of glass objects can also provide potentially useful information. Consider, for example, the extracted contours of two glasses in the upper left panel of Figure 15, and note in particular the oval shaped contour near the bottom of each glass that is formed at the boundary between the hollow top and the solid base. This is an especially powerful source of information that produces glass confidence ratings close to 100%, even when the background color is clearly inconsistent with that interpretation (e.g., see upper left panel of Figure 16). A similar type of solid/hollow boundary contour can also occur for uniformly hollow objects, provided that the glass shell is sufficiently thick so that its inner and

outer boundaries are perceptually distinct. A good example of that is shown in the upper middle image of Figure 15. The perceptual information from solid/hollow boundary contours could potentially explain why hollow objects are sometimes easier to identify as glass than solid ones (e.g., see Figures 11 and 12). Another type of contour within images of glass objects includes the swirling patterns we have referred to as eddies of light flow. These can occur in the peripheral shell of hollow objects, but they are larger and more prominent in solid ones. Flow eddies are particularly informative for bumpy surfaces such as the ones shown in Figures 1 and 8. They tend to form along the base of each bump, and this creates a kind of visual texture that is unique to bumpy glass objects.

In the present experiment, we attempted to demonstrate the perceptual relevance of these different types of contours by presenting them without any gray scale information, and comparing observers' judgments to a similar set of contour images derived from the reflections of opaque obsidian surfaces. This manipulation worked to some extent, in that the images derived from glass objects produced higher glass confidence ratings than the images derived from obsidian objects. However, two of the three contour images of obsidian objects were categorized primarily as glass, albeit with a relatively low confidence rating. This result is especially surprising given that the grayscale images of obsidian surfaces in Figures 6, 7, 8, 12, and 13 were all rated as shiny black with a high confidence level. This is clearly an issue that is deserving of future research.

Another diagnostic feature of glass materials that we did not explore in the present investigation is chromatic dispersion, which appears perceptually as bands of rainbow colors in an image. Because dispersion is unique to transparent materials, its presence in an image provides a potentially useful source of information. The materials used in the present experiment had relatively low dispersion, but the effect is clearly noticeable in many of our stimuli. It is interesting to note that this effect is typically turned off in many computer graphics applications in order to speed up rendering times, but this does not significantly impair the perceptual identification of glass objects. The chromatic structure of images can also facilitate the detection of solid/hollow boundary contours for objects composed of colored glass. Because solid regions absorb more light than hollow ones, the boundary between them can be accentuated by abrupt variations in brightness and saturation.

Still another powerful source of information for the perceptual identification of glass materials is provided by optical flow when an object is observed in motion. Tamura et al. (2018) have shown that observers can exploit differences in the patterns of optical flow between reflected and transmitted light in order to distinguish between glass and metal surfaces. This finding raises an interesting question about whether similar information is available when an object is viewed stereoscopically. When a surface is viewed from two different vantage points in binocular vision, the specular reflections in each view will generally be located at different surface locations, and the pattern of binocular disparities this creates may specify a 3D shape that is radically different from the ground truth (Blake & Bülthoff, 1990, 1991; Muryy, Welchman, Blake, & Fleming, 2013). Research has shown that stereograms of specular reflections are sometimes rivalrous, but in those cases where they are fusible, the stereograms subjectively enhance the appearance of gloss (Muryy, Fleming, & Welchman, 2016). The addition of transmitted light into the mix would seem to make the problem of stereo correspondence matching even more intractable. Although our experience with stereoscopic glass is rather limited, our informal observations are quite similar to those reported by Muryy et al. (2016): In some cases, the resulting stereograms are infusible and appear rivalrous. In others, they can be fused, and the fusion subjectively enhances the perception of glassiness. Figure 17 shows two examples in the latter category. The one on the top shows a stereoscopic version of the solid glass elephant from Figure 14, and the one on the bottom shows the hollow glass deformed sphere from Figure 7. Note in both cases how the presence of binocular disparity makes the glassiness of the depicted materials perceptually pop out.

One important issue we have not yet considered is what exactly observers are evaluating when they categorize a material as glass. In material science, glass is defined as a state of matter rather than a single material. It is typically created by heating silicon dioxide (i.e., sand) at a very high temperature until it melts, and then cooling it rapidly so that there is not enough time for a crystalline structure to form. Material scientists often refer to it as an amorphous solid, because it is a cross between a solid and a liquid with some of the properties of both. We usually think of glass as a man-made material, but it can also occur naturally. For example, obsidian is a form of glass that is created when molten rock from a volcano is cooled rapidly.

We suspect that most observers have no idea how glass is created, or the nature of its molecular structure. When they use that term to describe a material, they are most likely referring to the general category of things that are solid and transparent, of which physical glass is the most commonly observed exemplar. Note that there are many other materials that fit that general description, such as ice, diamond, cubic zirconia, and certain types of plastics, which can all be mistaken for glass if

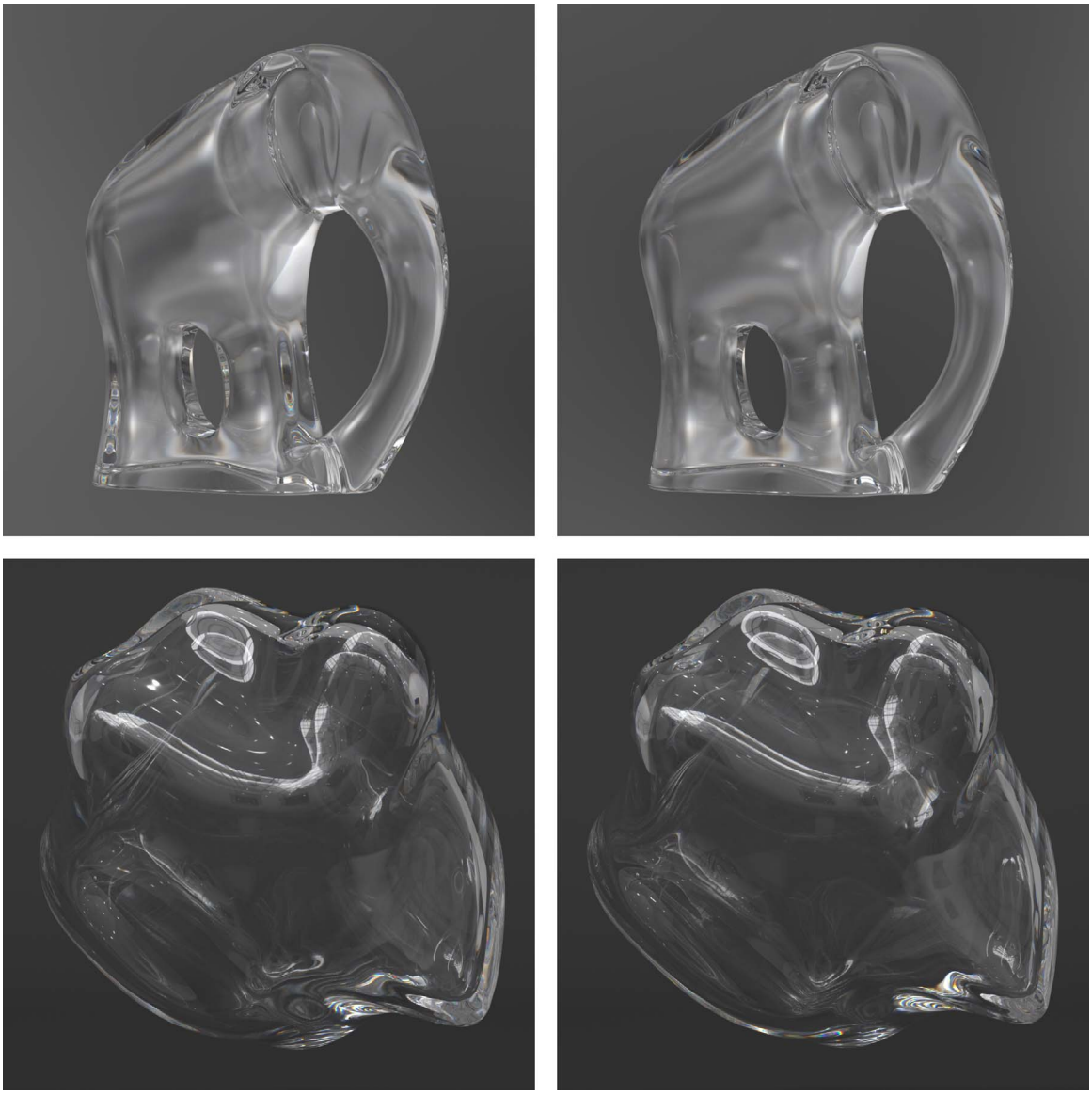

Figure 17. Stereograms of glass objects designed for crossed fusion. The top one is solid, whereas the bottom one is hollow.

viewed in the right context. Conversely, there are other glass materials such as obsidian that do not fit that general description, and are almost never identified as glass by naïve observers.

A similar misalignment between physical and perceptual categories can also occur with other types of materials. For example, there are many materials that reflect light in much the same way as obsidian, including onyx, shiny black plastic, and high gloss black paint. Because we do not have a convenient basic category term to describe those materials collectively, observers will often adopt the most common subordinate category to fill that role. For example, in free response tasks observers often describe our obsidian objects as black plastic, which is perfectly understandable given that they are optically indistinguishable.

Conclusions

The perceptual identification of glass is a complicated phenomenon. The present article describes several factors that can influence this process, including the structural complexity of an object, whether it is solid or hollow, the pattern of illumination, and the presence or absence of a background scene. We have also described a number of image features that are potentially diagnostic about glass materials, including flow eddies, contours that are formed at the boundary between hollow and solid regions, distortions of a background scene, chromatic dispersion, and patterns of optical flow. It is interesting to note that none of these sources of information are essential for the identification of glass, though some of them seem to be

sufficient. For example, solid/hollow boundary contours are a powerful source of information that can specify a transparent material even in a simple line drawing, but that information is only available when observing hollow objects. Similarly, distortions of a background scene can facilitate the identification of glass materials in some contexts, but most professional photographs of glass objects are shot against a uniform gray background. It is hoped that the present discussion will stimulate interest in this important aspect of material identification, and that it will provide motivation for future research.

Keywords: glass, transparency, material identification

Acknowledgments

This research was supported by a grant from the National Science Foundation (BCS-1849418).

Commercial relationships: none.
Corresponding author: James T. Todd.
Email: todd.44@osu.edu.
Address: Department of Psychology, Ohio State University, Columbus, OH, USA.

References

Beck, J., Prazdny, K., & Ivry, R. (1984). The perception of transparency with achromatic colors. *Perception & Psychophysics*, *35*, 407–422.

Blake, A., & Bülthoff, H. (1990, January 11). Does the brain know the physics of specular reflection? *Nature*, *343*(6254), 165–168.

Blake, A., & Bülthoff, H. (1991). Shape from specularities: Computation and psychophysics. *Philosophical Transactions of the Royal Society B: Biological Sciences*, *331*, 237–252.

Bousseau, A., Chapoulie, E., Ramamoorthi, R., & Agrawala, M. (2011, June). Optimizing environment maps for material depiction. In R. Ramamoorthi & E. Reinhard (Eds.), *Computer graphics forum* (Vol. 30, No. 4, pp. 1171-1180). Oxford, UK: Blackwell Publishing Ltd.

Doerschner, K., Boyaci, H., & Maloney, L. T. (2007). Testing limits on matte surface color perception in three-dimensional scenes with complex light fields. *Vision Research*, *47*, 3409–3423.

Fleming, R. W., & Bülthoff, H. (2005). Low-level image cues in the perception of translucent materials. *ACM Transactions on Applied Perception*, *2*, 346–382.

Fleming, R. W., Jäkel, F., & Maloney, L. T. (2011). Visual perception of thick transparent materials. *Psychological Science*, *22*, 812–820.

Hunter, F., Biver, S., & Fuqua, P. (2007). *Light, science & magic: An introduction to photometric lighting*. Amsterdam, the Netherlands: Elsevier.

Khan, E. A., Reinhard, E., Fleming, R. W., & Bülthoff, H. H. (2006, July). Image-based material editing. In J. Finnegan & H. Pfister (Eds.), *ACM Transactions on Graphics* (TOG) (Vol. 25, No. 3, pp. 654–663). ACM.

Kim, J., & Marlow, P. J. (2016). Turning the world upside down to understand perceived transparency. *i-Perception*, *2016*, 1–5.

Marlow, P. J., Kim, J., & Anderson, B. L. (2017). The perception and misperception of surface opacity. *Proceedings of the National Academy of Sciences, USA*, *114*, 13840–13845.

Metelli, F. (1970). An algebraic development of the theory of perceptual transparency. *Ergonomics*, *13*, 59–66.

Metelli, F. (1974). The perception of transparency. *Scientific American*, *230*, 90–98.

Motoyoshi, I. (2010). Highlight–shading relationship as a cue for the perception of translucent and transparent materials. *Journal of Vision*, *10*(9):6, 1–11, https://doi.org/10.1167/10.9.6. [PubMed] [Article]

Muryy, A. A., Welchman, A. E., Blake, A., & Fleming, R. W. (2013). Specular reflections and the estimation of shape from binocular disparity. *PNAS*, *110*, 2413–2418.

Muryy, A. A., Fleming, R. W., & Welchman, A. E. (2016). 'Proto-rivalry': How the binocular brain identifies gloss. *Proceedings of the Royal Society B: Biological sciences*, *283*:20160383, 1–9.

Norman, J. F., & Todd, J. T. (1996). The discriminability of local surface structure. *Perception*, *25*, 381–398.

Schlüter, N., & Faul, F. (2014). Are optical distortions used as a cue for material properties of thick transparent objects? *Journal of Vision*, *14*(14):2, 1–14, https://doi.org/10.1167/14.14.2. [PubMed] [Article]

Schlüter, N., & Faul, F. (2016). Matching the material of transparent objects: The role of background distortions. *i-Perception*, *7*(5), 1–24.

Singh, M., & Anderson, B. L. (2002). Toward a perceptual theory of transparency. *Psychological Review*, *109*, 492–519.

Tamura, H., Higashi, H., & Nakauchi, S. (2018). Dynamic visual cues for differentiating mirror and glass. *Scientific Reports*, *8*(1):8403, 1–12.

Todd, J. T., & Norman, J. F. (1995). The visual discrimination of relative surface orientation. *Perception*, *24*, 855–866.

Todd, J. T., & Norman, J. F. (2018). The visual perception of metal. *Journal of Vision*, *18*(3):9, 1–17, https://doi.org/10.1167/18.3.9. [PubMed] [Article]

Xiao, B., Walter, B., Gkioulekas, I., Zickler, T., Adelson, E., & Bala, K. (2014). Looking against the light: How perception of translucency depends on lighting direction. *Journal of Vision*, *14*(3):17, 1–22, https://doi.org/10.1167/14.3.17. [PubMed] [Article]